Article

Hydrophobin-Coated Perfluorocarbon Microbubbles with Strong Non-Linear Acoustic Response

Valentina Dichiarante [1], Giuseppina Salzano [1], Philippe Bussat [2], Emmanuel Gaud [2], Samir Cherkaoui [2] and Pierangelo Metrangolo [1,*]

[1] Department of Chemistry, Materials & Chemical Engineering "Giulio Natta", Politecnico di Milano, Via L. Mancinelli 7, 20131 Milano, Italy; valentina.dichiarante@polimi.it (V.D.); giusisalzano@gmail.com (G.S.)
[2] Bracco Suisse SA, Route de la Galaise 31, 1228 Plan-les-Ouates, Switzerland; philippe.bussat@bracco.com (P.B.); emmanuel.gaud@bracco.com (E.G.); samir.cherkaoui@bracco.com (S.C.)
[*] Correspondence: pierangelo.metrangolo@polimi.it

Abstract: Gas-filled microbubbles are well-established contrast agents for ultrasound imaging and widely studied as delivery systems for theranostics. Herein, we have demonstrated the promising potential of the hydrophobin HFBII—a fungal amphiphilic protein—in stabilizing microbubbles with various fluorinated core gases. A thorough screening of several experimental parameters was performed to find the optimized conditions regarding the preparation technique, type of core gas, HFBII initial concentration, and protein dissolution procedure. The best results were obtained by combining perfluorobutane (C_4F_{10}) gas with 1 mg/mL of aqueous HFBII, which afforded a total bubble concentration higher than 10^9 bubbles/mL, with long-term stability in solution (at least 3 h). Acoustic characterization of such microbubbles in the typical ultrasound frequency range used for diagnostic imaging showed the lower pressure resistance of HFBII microbubbles, if compared to conventional ones stabilized by phospholipid shells, but, at the same time, revealed strong non-linear behavior, with a significant harmonic response already at low acoustic pressures. These findings suggest the possibility of further improving the performance of HFBII-coated perfluorinated gas microbubbles, for instance by mixing the protein with other stabilizing agents, e.g., phospholipids, in order to tune the viscoelastic properties of the outer shell.

Keywords: hydrophobins; microbubbles; perfluorocarbons; phospholipids; ultrasound imaging

1. Introduction

Gas-filled microbubbles (MBs) consist of a gaseous core—usually composed of oxygen, sulfur hexafluoride (SF_6) or perfluorocarbons (PFCs)—coated with a biocompatible shell of lipids, proteins or other biocompatible macromolecules, with diameters ranging from 0.1 to 10 μm [1]. Due to their unique features such as inertness, stability and echogenic properties, MBs hold huge importance for ultrasound (US) biomedical applications, such as blood-pool contrast agents (CAs) for US imaging or targeted drug delivery [2]. Indeed, the compressibility of their gas cores generates volumetric oscillations in response to US fields and, thus, enhances the harmonic echoes produced by living tissues [3]. These CAs are nowadays widely used for clinical diagnosis, in particular for echocardiography and radiology [4,5], but have also found application as molecular imaging tracers for the targeting of specific cellular biomarkers of diseases, as well as vehicles for the efficient delivery of therapeutic molecules, ranging from small drugs to genes [6–10]. This is due to the fact that their oscillations may induce deformations and the temporary opening of pores into cell membranes, thus increasing permeability [11,12]. Besides their medical uses, gaseous MBs are also under study for analytical purposes, including acoustic detection, microfluidic analysis, electrochemical sensing, and the application of mass transport behavior at gas/liquid interfaces in gas sensing or biosensing [13].

The combination of the peculiar properties of MBs with the cost-effectiveness, non-invasive character, portability, and versatility of US-based techniques accounts well for their successful rise, and the absence of ionizing radiation explains their wide acceptance for pediatric uses [14]. Obviously, both diagnostic and therapeutic uses of MBs require the optimization of their stability and performance in terms of echogenicity, shell rigidity and clearance efficiency. All these properties depend on the composition and thickness of the coating shell, as well as on the type of core gas [15,16]. To increase stability in biological fluids and prolong their lifetimes, typically, microbubbles are filled with high-molecular-weight gases with low aqueous solubility, such as SF_6 and PFCs. Further improvements of MBs' stability in the bloodstream can be achieved by using different coating materials for their stabilizing shell, including polymers, proteins, nanoparticles, and, more often, phospholipids, or PEGylated lipids, which were found to allow a longer in vivo circulation time [17–19]. Several approaches were developed for the preparation, as well as for the physico-chemical and acoustic characterization, of this latter family of US-responsive CAs [20]. Significant examples in this field are Sonovue®, a commercially available phospholipid-coated SF_6-containing MB system used in diagnostic imaging, and Definity®, a lipid-coated MB system composed of perfluoropropane (C_3F_8), which has been approved by the Food and Drug Administration (FDA) for echocardiography [4]. Compared to air-filled bubbles, both formulations have smaller diameters (about 2.5–4 µm), which facilitate their passage through pulmonary capillaries and, thus, increase the blood flow imaging time. Another interesting example of commercially available US-responsive CA is Optison®, consisting of C_3F_8 encapsulated in a human serum albumin shell [21].

An ideal MB formulation for biomedical applications should actually fulfill the following requirements: (i) easy preparation; (ii) high concentration (at least 10^7 MBs/mL); (iii) small and controlled size, to avoid filtration by the lungs; (iv) long storage stability in solution; and (v) high echogenicity, resistance to bloodstream pressure, and clearance efficiency [1]. Up to now, commercially available MBs have only partially met these criteria. Some phospholipid-coated MBs, for instance Sonovue, have a thin and highly echogenic shell and can be freeze-dried for extending their shelf-life, facilitating storage and transportation. At the same time, they need to be reconstituted from lyophilized materials just prior to use, thus increasing production costs. More convenient alternatives are those CAs that can be simply resuspended by mechanical shaking or even by hand mixing, as in the cases of Definity and Optison, respectively. On the other hand, polymer-shelled MBs can be stored for months and have thicker shells that might be useful for drug encapsulation and delivery. Unfortunately, increased shell thickness considerably decreases echogenicity at low US pressures while prompting bubble breakage and gas release at high acoustic pressures [15].

In the search for alternative and more effective formulations, we focused on the use of hydrophobins (HFBs), small fungal amphiphilic proteins, as biocompatible self-assembling coating materials for gas-filled MBs [22,23]. Among them, we selected HF-BII, obtained from *Trichoderma reesei*, which is known to form highly ordered layers at hydrophilic–hydrophobic interfaces, lowering surface tension and helping the dispersion of several insoluble materials in water [24,25]. Recently reported applications of HFBII include the stabilization of food foams and emulsions [26,27], targeted and controlled delivery of drugs [28–32], dispersion of highly hydrophobic polymeric nanoparticles in water [33], and stabilization of fluorocarbon emulsions [34–36]. Interestingly, recent studies have showed that multiple compression and expansion cycles have a major influence on the morphology of HFBII air–water interfacial structures, proving that the protein layers tend to become more homogeneous when compressed and expanded several times [37]. Furthermore, some of us have previously demonstrated the exceptional ability of HFBII aqueous solutions, previously saturated with perfluorohexane (C_6F_{14}) gas, to be formed by shear mixing spherical and monodisperse MBs, which were stable in dispersion at room temperature for at least 3 months [38].

The aim of this study was to further investigate the potential of HFBII as a coating shell for gas-filled MBs (herein labeled as HFBII-MBs, Figure 1), suitable as US imaging CAs. In particular, its MB-coating performance was tested for the first time with two perfluorinated core gases already approved for clinical use, namely SF_6 and perfluorobutane (C_4F_{10}). The results were compared with those obtained with nitrogen, as a reference non-fluorinated core gas. Several experimental parameters were thoroughly studied, including different starting concentrations of HFBII solutions, the effect of preliminary headspace saturation with gaseous C_6F_{14}, and the use of alternative preparation methods, in order to find the best conditions for obtaining MBs at high concentrations and with a relatively high stability in solution. Finally, the resistance to high pressures and acoustic properties of HFBII-MBs were investigated in detail to evaluate their potential for in vivo application.
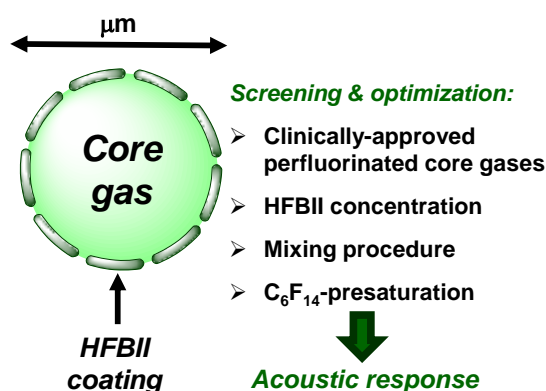

Figure 1. Schematic structure of a HFBII-MB and summary of the performed experimental screening.

2. Materials and Methods

HFBII was kindly provided by VTT Biotechnology (VTT Technical Research Center of Finland, Finland). Nitrogen was purchased from Carbagas (Gumigen, Switzerland). Sulfur hexafluoride (SF_6) was purchased from Scott Medical Product (Plumsteadville, PA, USA). Octafluoropropane (C_3F_8) and decafluorobutane (C_4F_{10}) were provided by F2 Chemicals (Lancashire, UK). Tetradecafluorohexane (C_6F_{14}) was supplied by Sigma Aldrich (Sigma-Aldrich, Taufkirchen, Germany), and C_6F_{14}-saturated nitrogen was prepared using a Tedlar Bag (Blanc labo, Lonay, Switzerland).

2.1. Preparation of HFBII Aqueous Solutions

HFBII solutions were prepared by dissolving 2 mg or 10 mg of HFBII in 10 mL of Milli-Q water in a glass vial. The resulting dispersions (HFBII concentration: 0.2 or 1 mg/mL, respectively) were gently hand-shaken and introduced in a sonicating bath (Branson 5200) for 15 min. Solutions were then sampled in DIN8R injection vials (5 mL/vial). The vials were sealed, and the vial headspace was replaced by C_6F_{14}-saturated nitrogen. Then, they were placed on the rotator at 22 rpm for two hours. HFBII solutions without C_6F_{14}-saturation were used as control tests.

2.1.1. Preparation of MBs via the Vialmix™ Method

HFBII solutions were sampled in DIN2R injection vials (1 mL/vial), followed by the addition to the headspace of the vial of the desired core gas (namely, N_2-, SF_6-, C_4F_{10}- or C_6F_{14}-saturated nitrogen). The same procedure was also performed for HFBII solutions previously flushed with C_6F_{14}-saturated nitrogen. In all cases, the vials were then stoppered, sealed and stirred on a Vialmix™ apparatus (Lantheus Medical Imaging Inc., North Billerica, MA, USA) for 45 s. The obtained MB suspensions were kept for 10 min at room temperature. Finally, the vials were gently hand-shaken to allow MB homogenization before analysis.

2.1.2. Preparation of MBs via the Polytron Method

HFBII solutions (1.5 mL) were placed in 5 mL polypropylene tubes, and the headspace was saturated with the desired core gas. The Polytron head (Polytron PT3100 -DA 07/2 EC-B101, Kinematica) was then inserted into the tube while constantly flushing its headspace with the selected core gas. Solutions were mixed at 12,000 rpm for 45 s, and then at 20,000 rpm for further 45 s. The tubes were stoppered, and the obtained MB suspensions were kept for 10 min at room temperature. Finally, the tubes were gently hand-shaken to allow MB homogenization before analysis.

2.1.3. Decantation of MBs

Suspensions of HFBII-coated MBs, prepared via the Vialmix™ method, were diluted with 6 mL of distilled water and put in 10 mL syringes. Each syringe was placed horizontally for 1 min, then the infranatant was recovered and transferred in another 10 mL syringe. After keeping the second syringe horizontal for 2 min, the infranatant was again collected and transferred in another 10 mL syringe. This last step was repeated once more, before transferring the resulting MB suspension to a DIN8R vial. Finally, the vial's headspace was filled with the appropriate gas, and the vial was stoppered and sealed.

2.2. Size Distribution and Concentration

Size distributions and concentrations of MBs were assessed using a Coulter counter Multisizer 3 (Beckman Coulter, Fullerton, CA, USA) fitted with a 30 μm aperture tube. Samples were diluted from 50- to 200-fold with 0.9% aqueous sodium chloride before analysis. MBs were characterized by measuring their mean diameter and both number- and volume-averaged (DN and DV, in μm), with their total concentration expressed as the number of MBs/mL and the concentration of bubbles with sizes in the clinically useful range (2–8 μm).

2.3. Optical Microscopy Analysis

MB suspensions were drop-cast on a glass slide, covered with a coverslip, and then observed via optical microscopy, using a Leitz DMRBE Microscope (Leica Microsystems, Heerbrugg, Switzerland).

2.4. Pressure Resistance Measurements

The resistance of MBs to pressure was evaluated using an in-house-developed pressure nephelometer by measuring absorbance (Spectrophotometer Jenway 6300, Cole Parmer, Vernon Hills, IL, USA) as a function of increased hydrostatic pressure. Samples were diluted 20 times with 0.9% aqueous sodium chloride. The Pc50 value, corresponding to the hydrostatic pressure reached at 50% of the initial absorbance, was then extrapolated.

2.5. Spectral Attenuation Measurements

The spectral acoustic response of MBs, i.e., their acoustic response as a function of the frequency, was measured using spectral attenuation measurements [39]. A diluted suspension of MBs (1:500) was prepared in a home-made cell placed in a water tank. A broadband transducer (Panametrics 7.5 MHz unfocused, Evident Corporation, Tokyo, Japan) was used to transmit broadband acoustic pulses (2–13 MHz) and record echo responses after propagation through the microbubbles' suspension. A Pulser/Receiver (Panametrics 5900PR, Evident Corporation, Tokyo, Japan) was used to drive the transducer and amplify echo signals, which were then recorded on a digital oscilloscope (LeCroy HRO 64Zi, Teledyne Technologies, Chestnut Ridge, NY, USA). The resulting attenuation spectra were the average of 30 acquisitions. Finally, a MATLAB (The MathWorks, Natick, MA, USA) script was written to calculate attenuation spectra by comparing the signals received in the presence of MBs with those transmitted by an acoustically transparent reference solution. The energy levels of the Pulser/Receiver allowed us to measure acoustic pressures ranging from 18 to 187 kPa.

2.6. Harmonic Response

In addition to broadband measurements, MBs' acoustic responses were also assessed using narrowband pulses (single frequency) in order to reveal their potential ability to generate harmonic and/or subharmonic (nonlinear) echoes. For these experiments, the MB suspension (diluted 1:1000) was insonified with a narrowband pulse at 5 MHz, using a focused transducer (Panametrics 5 MHz, focal distance = 3″, Evident Corporation, Tokyo, Japan). The latter was driven by an Arbitrary Waveform Generator (Tabor 8014, Tabor Electronics, Nesher, Israel) generating a 5 MHz 50-cycle burst, amplified by an RF amplifier (ENI 3200L, Electronics and Innovation Ltd, Rochester, NY, USA). The backscatter spectra were the average of 50 acquisitions. The content of the measurement cell was renewed for each acoustic pressure and stirred permanently. Backscattered echoes were received by a second focused transducer (Vermon M3, Vermon, Tours, France), which was confocally aligned with the first one. The receiving transducer showed a sensitivity bandwidth sufficient to acquire both the fundamental response F (5 MHz) and the subharmonic F/2 response (2.5 MHz) of MBs. The resulting signals were amplified by a Pulser/Receiver (Panametrics 5900PR) and recorded on a digital oscilloscope (LeCroy HRO 64Zi). Finally, a MATLAB script was written to compute the backscatter power spectra acquired at acoustic pressures between 20 and 150 kPa.

3. Results and Discussion

3.1. Influence of Different Core Gases and HFBII Dissolution Procedures

As a first step, we decided to compare sizes and morphologies of MBs obtained using aqueous solutions of HFBII prepared with and without a C_6F_{14}-saturated atmosphere. According to the preliminary results reported by Gazzera et al. [38], the saturation of HFBII solutions with vapors of perfluorohexane allowed for a better dispersion of the protein in aqueous media. We definitively confirmed that, after 3 h of mixing at 22 rpm under a nitrogen atmosphere, HFBII formed a milky dispersion of fibrils in water, as observed via optical microscopy (Figure S1a). These fibrils tended to float, supporting the hypothesis that they were gas-filled. In contrast, when the headspace of the vial, containing either 0.2 or 1 mg/mL of HFBII in water, was flushed with C_6F_{14}-saturated nitrogen gas under the same mixing conditions, clear solutions were obtained. Dynamic Light Scattering (DLS) measurements of such solutions showed a mean particle diameter of about 550 nm (Figure S1b), which was significantly higher if compared to the previously reported one ($\approx$ 10 nm), probably due to the higher mixing rate (250 rpm) used in that case [38].

Besides the nature of the shell, an appropriate choice of core gas is of paramount importance for the improvement of MBs' stability, with high-molecular-weight inert gases and perfluorinated gases usually giving better results. We evaluated the effects of various gases on MB size distribution, concentration, short-term stability after preparation and longer-time storage at room temperature. At the same time, we assessed the influence exerted by the two types of HFBII solutions (prepared with or without preliminary saturation with C_6F_{14}, respectively), as well as of different concentrations of the protein.

In this first part of the study, mechanical shaking (Vialmix™ method, see Section 2 for details) was used to prepare HFBII-shelled MBs filled with various gases. Two sets of experiments were carried out: in the former, we used milky HFBII solutions prepared under a nitrogen atmosphere, whereas in the latter, we started from clear HFBII solutions previously saturated with C_6F_{14} vapors. In both cases, 0.2 mg/mL HFBII solutions were sampled into injection vials (1 mL/vial), and the headspace of each vial was filled with the selected core gas, namely nitrogen, SF_6, C_4F_{10}, or C_6F_{14}-saturated nitrogen. The resulting MB suspensions were characterized 10 min and 3 h after preparation (Table 1 and Figure 2).

Table 1. Mean diameter, both number- and volume-averaged (DN and DV, in μm); total concentration expressed as the number of MBs/mL; concentrations of MBs with sizes in the clinically useful range (2–8 μm); and pressure resistance (Pc50) of HFBII-MBs prepared using the Vialmix™ method, starting from either N_2-saturated or C_6F_{14}-saturated HFBII solutions (0.2 mg/mL) and different core gases.

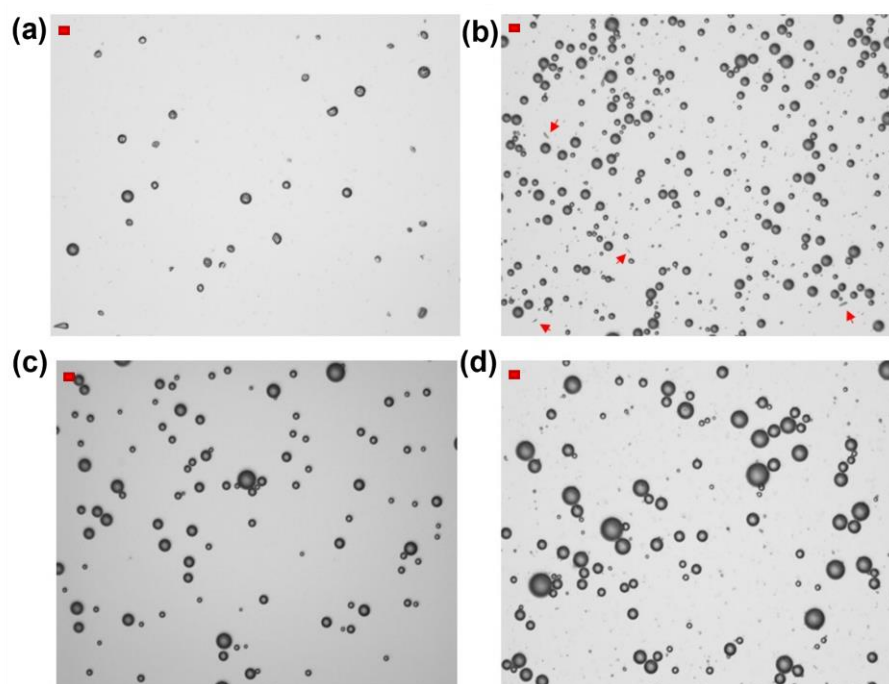| Headspace Gas	Core Gas	Time after Activation (min)	DV (μm)	DN (μm)	Total MBs/mL ($\times 10^6$)	<2–8 μm> MBs/mL ($\times 10^6$)	Pc50 (mmHg)
N_2	N_2	10	12	1.4	40.0	2.2	50
		180	n.d.	n.d.	n.d.	n.d.	n.d.
	SF_6	10	12	2	70.0	9.4	56
		180	12	2.4	62.0	9.6	84
	C_4F_{10}	10	14	1.5	220.0	11.5	76
		180	14	1.6	224.0	13.0	72
	C_6F_{14}-saturated N_2	10	14	5	19.0	2.4	81
		180	13	5	21.0	3.7	115
C_6F_{14}	N_2	10	11	1.6	135.3	22.1	n.d.
		180	10	2	94.4	21.4	113
	SF_6	10	12	1.8	174.0	22.3	n.d.
		180	12	2	106.3	23.3	110
	C_4F_{10}	10	14	1.4	214.3	14.2	n.d.
		180	14	1.5	217.1	15.8	118
	C_6F_{14}-saturated N_2	10	12	1	18.1	0.4	n.d.
		180	12	1	21.6	0.2	n.d.

Figure 2. Optical microscope images of HFBII-MBs prepared from N_2-saturated HFBII solutions (0.2 mg/mL) and filled with different core gases: (**a**) nitrogen; (**b**) SF_6; (**c**) C_6F_{14}-saturated nitrogen; (**d**) C_4F_{10} (scale bars, in red, top left: 10 μm). The red arrows in Figure 2b highlight the presence of fibrils.

Using HFBII starting solutions not saturated with C_6F_{14} and nitrogen as the core gas, MBs were obtained at a relatively low total concentration of about 4×10^7 MBs/mL, and

almost 20 times lower if we counted only particles with diameters in the range of 2–8 μm, which is the optimal interval for biomedical applications. As shown in Figure 2a, according to optical microscopy analysis, these HFBII-MBs were mostly spherical and possessed a wrinkled shell, which according to a recently reported study could be attributed to the effect of compressive stress on the protein film [40]. Unfortunately, they showed a limited stability at room temperature, and after 3 h, a clear solution was observed, with no particles detected via Coulter counter analysis. Compared to nitrogen, the use of SF_6 as the core gas under the same conditions led to a slight increase in concentration, up to 7×10^7 MBs/mL, but with a larger size distribution. As shown in Figure 2b, the majority of SF_6-filled HFBII-MBs were spherical, with a few fibrils still present in the dispersion (highlighted by red arrows in the image). In contrast to the nitrogen-containing ones, these MBs were stable for at least 3 h after preparation, in terms of both size and concentration. The use of C_6F_{14}-saturated nitrogen as the core gas produced spherical MBs at the lowest concentration (only 2×10^7 MBs/mL) but with a narrower size distribution compared to the other gases (Figure 2c). Interestingly, when HFBII-MBs were prepared using C_4F_{10} as the core gas, the highest concentration of MBs was achieved (about 2×10^8 MBs/mL), characterized by a spherical shape and a broad size distribution (Figure 2d). As observed for their SF_6 counterparts, perfluorobutane-filled HFBII-MBs were stable for at least 3 h after preparation, with no detectable changes in particle size and concentration.

The same set of experiments was then repeated using clear HFBII solutions, prepared under a perfluorohexane-saturated atmosphere. Table 1 and Figure 3 show their detailed characterization. Compared to the previous series of HFBII-MBs, the use of both SF_6 and nitrogen cores led to an increase in MBs concentrations and a more spherical shape. Notably, N_2-filled MBs became more stable and were still detectable 3 h after preparation. In contrast, MBs filled with C_6F_{14}-saturated nitrogen were characterized by a very low total concentration ($\approx 2 \times 10^7$ MBs/mL), which was even 50 times lower for bubbles in the 2–8 μm size range (4×10^5 MBs/mL). When C_4F_{10} was used as the filling gas, the preliminary saturation of HFBII solution with C_6F_{14} seemed to have almost no influence, and the resulting total MB concentration was again close to 2×10^8 MBs/mL.
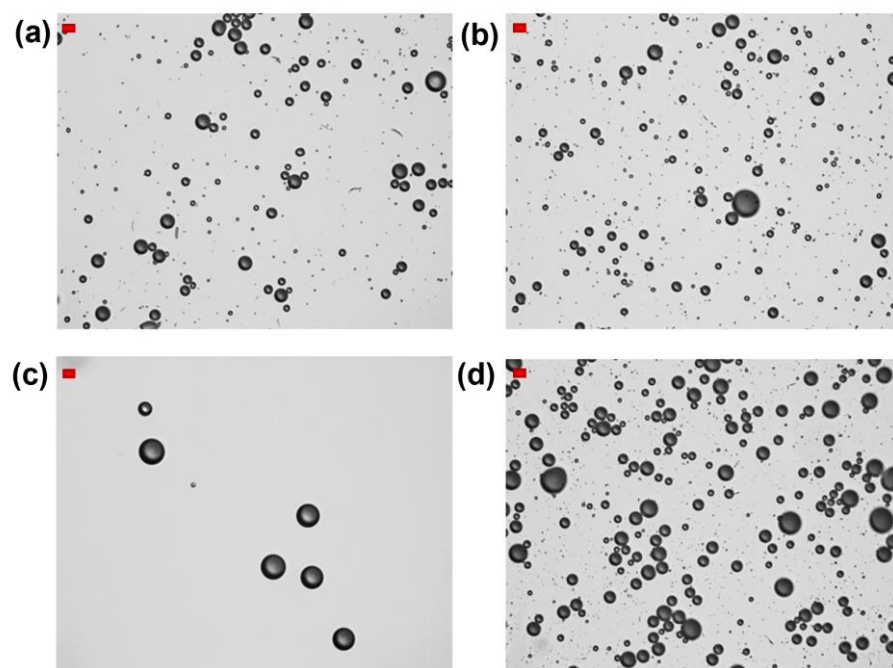

Figure 3. Optical microscope images of HFBII-MBs prepared using C_6F_{14}-saturated HFBII solutions (0.2 mg/mL), and filled with different core gases: (**a**) nitrogen; (**b**) SF_6; (**c**) C_6F_{14}-saturated nitrogen; (**d**) C_4F_{10} (scale bars, in red, top left: 10 μm).

In summary, the data reported above confirmed that the preliminary saturation of HFBII solutions with perfluorohexane vapors allowed the more efficient dispersion of the protein in water but had a limited influence on the final concentration and stability in solution of HFBII-MBs filled with PFC gases. On the other hand, this treatment could afford improved results in the case of N_2- or SF_6-containing MBs. Among all the selected core gases, the highest MB concentration was obtained using perfluorobutane, whose MBs were found to be stable for at least 3 h at room temperature in solution.

We then evaluated the resistance of the different HFBII-MBs to pressure (Pc50) via UV measurements (Table 1). In all cases, pressure resistance was not significantly affected by the nature of the core gas and by the initial procedure used for dissolving HFBII in water (with or without C_6F_{14}-saturation). However, compared to phospholipid-shelled MBs, which have a pressure resistance compatible for the in vivo use of ≈100 mmHg using N2 and ≈800 mmHg using C_4F_{10} [41], HFBII-shelled MBs were characterized by a low-pressure resistance in all the tested conditions, with values ranging from 50 to 118 mmHg. Such reduced resistance could be a limitation for the in vivo use of HFBII-MBs, since they might not survive systolic pressure after intravenous injection and, thus, require further optimization studies.

3.2. Influence of HFBII Initial Concentration

In a first attempt at increasing their pressure resistance, we decided to prepare HFBII-MBs starting from a higher HFBII concentration (1 mg/mL). In this set of experiments, HFBII solutions were prepared under N_2 atmosphere, without saturation with perfluorohexane, and only perfluorinated filling gases were tested. Table 2 reports the results achieved, which should be compared to those obtained using HFBII at a 0.2 mg/mL initial concentration (Table 1). For all the selected core gases, the size distribution of HFBII-MBs was quite broad, whereas the mean number-averaged diameter (DN) was lower, with a higher number of smaller MBs, if compared to analogous samples prepared from 0.2 mg/mL HFBII solutions. Interestingly, the use of a higher concentration of HFBII led to a significant increase in the microbubbles' concentrations. In particular, SF_6- and C_4F_{10}-containing HFBII-MBs showed a total concentration about 8- to 10-fold higher when starting from 1 mg/mL HFBII if compared to 0.2 mg/mL of protein, reaching a value of ≈2.5×10^9 MBs/mL in the case of perfluorobutane core gas. In both cases, the concentrations of MBs in the 2–8 μm size range became about 7-fold higher. Much less satisfying were the data obtained when using C_6F_{14}-saturated nitrogen as filling gas, since the increase in both concentrations was significantly lower. Despite the promising results in terms of the concentrations and sizes of HFBII-MBs, the use of a higher initial concentration of protein did not lead to decisive improvements of their pressure resistance, which remained, in all cases, below 100 mmHg.

Table 2. Mean diameter, both number- and volume-averaged (DN and DV, in μm); total concentration expressed as number of MBs/mL; concentration of MBs with sizes in the clinically useful range (2–8 μm); and pressure resistance of HFBII-MBs prepared via the Vialmix™ method, starting from N_2-saturated HFBII solutions (1 mg/mL) and different fluorinated core gases.

Core Gas	Time after Activation (min)	DV (μm)	DN (μm)	Total MBs/mL ($\times 10^6$)	<2–8 μm> MBs/mL ($\times 10^6$)	Pc50 (mmHg)
SF_6	10	12	2	573.0	64.9	86
	180	12	2	604.0	55.0	81
C_4F_{10}	10	12	1	2541.0	85.6	64
	180	12	1	2324.0	72.8	73
C_6F_{14}-saturated	10	14	2	50.0	3.5	85
N_2	180	14	2	69.0	3.5	79

3.3. Comparison between the Vialmix™ and Polytron Preparation Methods

Finally, we evaluated the effects of different preparation procedures on the characteristics of the resulting HFBII-MBs by comparing the Vialmix™ and Polytron methods. The

former is a device specifically designed for the activation of Definity® samples through mechanical agitation, under a controlled shaking rate and duration, of a solution of the shell material in a sealed vial with the headspace filled with the core gas. The latter is an immersion homogenizer that exploits the shear force of its tip to form MBs via rotor/stator homogenization [42]. To be precise, the Polytron dispersion procedure previously reported by Gazzera et al. [38] was slightly modified and adapted to the smaller volumes of HFBII solutions used in the current work. Table 3 shows the results obtained via this optimized procedure. As reported in Table 3, with SF_6-filled HFBII-MBs prepared starting from 0.2 mg/mL of protein, the Polytron method gave a higher total MB concentration than the Vialmix™ one, but a similar value in the 2–8 μm size range. With a 1 mg/mL initial HFBII, the MBs' concentrations increased only 2-fold, whereas the improvement obtained with Vialmix™ was significantly higher (up to 7–10-fold). A similar trend was observed with C_4F_{10} core, with a very low increase in concentration when going from 0.2 to 1 mg/mL of protein. With C_6F_{14}-saturated nitrogen, both methods gave only slight increases in the microbubbles' concentrations (around 2-fold), especially for particles in the 2–8 μm range. These data allowed us to conclude that Vialmix™ is a simpler and more easily scalable method for preparing HFBII-MBs filled with perfluorinated gases.

Table 3. Mean diameter, both number- and volume-averaged (DN and DV, in μm); total concentration expressed as number of MBs/mL; and concentrations of MBs with sizes in the clinically useful range (2–8 μm) of HFBII-MBs prepared via the Polytron method, starting from N_2-saturated HFBII solutions (either 0.2 or 1 mg/mL) and different core gases.

Core Gas	[HFBII] (mg/mL)	DV (μm)	DN (μm)	Total MBs/mL ($\times 10^6$)	<2–8 μm> MBs/mL ($\times 10^6$)
SF_6	0.2	12	1	138.8	7.3
	1	13	1	247.7	11.2
C_4F_{10}	0.2	10	2	349.0	61.3
	1	11	1	377.9	22.7
C_6F_{14}-saturated N_2	0.2	8	1	70.6	2.9
	1	14	2	89.5	7.0

3.4. Echogenicity and Acoustic Characterization of HFBII-Shelled Microbubbles

The acoustic response of HFBII-MBs was investigated using bubbles filled with perfluorobutane gas only, because they were obtained at the highest concentration. Since acoustic characterization requires MBs with a narrower size distribution, HFBII-MBs prepared via the Vialmix™ method were subjected to a decantation procedure, as described in Section 2.1.1. As a result, aggregates larger than 8 μm were almost completely removed, without affecting the concentrations of MBs in the 2–8-μm size range. To confirm the stability of bubbles, before performing acoustic measurements, the size distribution was measured immediately after preparation (t0) and after overnight storage in solution (t0 + 18 h). As shown in Figure S2, these measurements revealed the existence of a stabilization period, with a change in size distribution over time due to the loss of both the smallest and the largest bubbles. Acoustic measurements were then performed 18 h after preparation in order to let MBs stabilize and reach their final size, using the frequency range typical of diagnostic ultrasound imaging (2–12 MHz).

The spectral acoustic response of the HFBII-shelled MBs, defined as their acoustic response as a function of frequency, was measured via spectral attenuation experiments. This technique consists of measuring the attenuation coefficient of US waves that propagate through a bubble dispersion as a function of time for a certain range of US frequencies. A strong acoustic response leads to a strong attenuation of the acoustic waves due to absorption and backscatter of their energy by the sample. A first series of attenuation measurements was performed at a low acoustic pressure (18 kPa Peak Negative Pressure), at which HFBII-MBs oscillate in their elastic regime, on a sample of microbubbles diluted 500 times, by repeating the measurement several times over a period of 20 min (Figure 4a). Generally, the attenuation spectrum is expected to show a peak at the microbub-

ble resonance frequency, i.e., the frequency of its maximum response, which is inversely proportional to the MB size. In our case, given the small size of HFBII-MBs, the resonance peak was located at a very high frequency, out of the transducer bandwidth. Interestingly, these measurements showed the excellent stability of the acoustic response over time, in a diluted sample, with a small drift appearing only after 20 min.
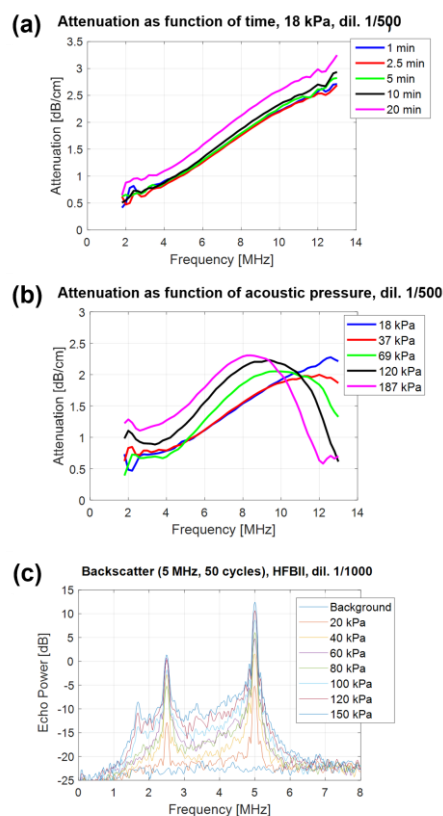

Figure 4. Acoustic response of C_4F_{10}–filled HFBII–MBs: (**a**) attenuation spectra of HFBII–MBs (diluted 1:500), measured at 18 kPa as a function of time over 20 min; (**b**) attenuation spectra of HFBII–MBs (diluted 1:500), measured at increasing values of acoustic pressure; (**c**) backscatter power spectra of C_4F_{10}–filled HFBII–MBs (diluted 1:1000) as a function of acoustic pressure.

A second series of attenuation measurements was performed by varying the acoustic pressure from 18 up to 187 kPa (Figure 4b). The resulting data showed the strong acoustic pressure dependence of the MB response, with a shift of about 4 MHz in the resonance peak toward lower frequencies when increasing the pressure. Interestingly, since the size distribution did not change significantly, the shift in resonance peak could be attributed to the strong non-linear behavior of the HFBII-MBs. This means that their viscoelastic shell parameters were not constant but depended on the oscillation amplitude. As a result, our MBs appeared less stiff when the oscillation amplitude increased, as already reported by Segers et al. for phospholipid-stabilized microbubbles [43].

3.5. Harmonic Response of HFBII-MBs

In addition to previous attenuation measurements performed using broadband acoustic pulses (2–12 MHz), the acoustic response of HFBII-MBs was also assessed using narrowband pulses (single frequency) in order to investigate their potential ability to generate harmonic echoes. Backscatter power spectra were measured at different acoustic pressures, between 20 and 150 kPa, and the results are shown in Figure 4c. When oscillating, our microbubbles scattered energy not only at the excitation frequency F but also at the different harmonic frequencies (F/3, F/2, 2F, 3F, 4F, etc.). In addition to a strong subharmonic response (F/2) that was already present at low acoustic pressures (20 kPa), a subharmonic

response at F/3 appeared at 100 kPa. These experiments also allowed us to measure the level of acoustic broadband noise, which is due to MB destruction. For HFBII-MBs, this level was between 3 and 4 MHz and exceeded the background level starting from 40 kPa, indicating that at this acoustic pressure, these MBs were already starting to be destroyed, differently from the higher values generally observed for phospholipid-stabilized MBs.

From all of the above results, it appears clearly that HFBII can easily form stable PFC microbubbles in high concentrations and with strong non-linear acoustic responses, but if used alone as stabilizing shell, it does not provide sufficient pressure resistance for in vivo US imaging. To overcome this issue, a viable strategy could be to mix HFBII with other amphiphiles, e.g., phospholipids, thus combining the advantages of different coating agents. This approach, for instance, proved to be successful for mixed coating monolayers of semifluorinated alkanes and phospholipids, showing linear and non-linear viscoelastic properties comparable to those of phospholipids alone, but strongly improved stability [44].

4. Conclusions

In summary, stable HFBII-shelled gaseous MBs were easily obtained at good concentrations using a commercially available mechanical shaker apparatus, and subsequent decantation allowed the effective removal of larger MBs (>8 μm), narrowing their size distribution. The saturation of HFBII starting solutions with perfluorohexane vapors actually afforded clear dispersions of this amphiphilic protein and improved the stability of the resulting MBs when nitrogen or SF_6 were used as core gases. On the other hand, if PFC gases were used to fill HFBII-MBs, such preliminary treatment did not greatly affect the outcome. Overall, the best results were achieved using C_4F_{10} gas in combination with 1 mg/mL of HFBII, leading to a total bubble concentration higher than 10^9 MBs/mL and long-term stability in solution (at least 3 h).

Regarding the acoustic responses of perfluorobutane-filled HFBII-MBs, the performed studies proved that dilution had no effect on their performance during the first 10 min, suggesting the effective and reproducible echogenic properties of these MBs. However, if compared to conventional MBs stabilized by phospholipid shells, the pressure resistance of HFBII-MBs was found to be lower, and under ultrasound exposure destruction signals were recorded already starting from 40 kPa. Interestingly, C_4F_{10}-filled HFBII-MBs showed a strong non-linear behavior, and their harmonic response was already substantial at acoustic pressures as low as 20 kPa.

These findings suggest that, although HFBII alone may not fulfill all the requirements needed for in vivo US imaging, nevertheless, its ability to generate easy-to-prepare MBs at high concentrations, with small sizes and long stability in solution, should be taken into consideration for further investigations. In particular, the introduction of other excipients or surfactants in the shell of MBs together with HFBII could increase the stability of the coating layer under high pressures while maintaining the specific advantages provided by this protein.

Supplementary Materials: The following supporting information can be downloaded via this link: https://www.mdpi.com/article/10.3390/chemistry6020016/s1, Figure S1: effect of C_6F_{14}-saturated atmosphere on the dissolution of HFBII in water; Figure S2: size distribution analysis of C_4F_{10}-filled HFBII-MBs at different times after production.

Data Availability Statement: The raw data supporting the conclusions of this article will be made available by the authors on request.

Conflicts of Interest: The authors declare no conflicts of interest.

References

1. Upadhyay, A.; Dalvi, V. Microbubble formulations: Synthesis, stability, modeling and biomedical applications. *Ultrasound Med. Biol.* **2019**, *45*, 301–343. [CrossRef] [PubMed]

2. Navarro-Becerra, J.A.; Borden, M.A. Targeted Microbubbles for Drug, Gene, and Cell Delivery in Therapy and Immunotherapy. *Pharmaceutics* **2023**, *15*, 1625. [CrossRef] [PubMed]

3. Roovers, S.; Segers, T.; Lajoinie, G.; Deprez, J.; Versluis, M.; De Smedt, S.C.; Lentacker, I. The role of ultrasound-driven microbubble dynamics in drug delivery: From microbubble fundamentals to clinical translation. *Langmuir* **2019**, *35*, 10173–101917. [CrossRef]

4. Yusefi, H.; Helfield, B. Ultrasound Contrast Imaging: Fundamentals and Emerging Technology. *Front. Phys.* **2022**, *10*, 791145. [CrossRef]

5. Kuriakose, M.; Borden, M.A. Microbubbles and nanodrops for photoacoustic tomography. *Curr. Opin. Colloid Interface Sci.* **2021**, *55*, 101464. [CrossRef]

6. McMahon, D.; O'Reilly, M.A.; Hynynen, K. Therapeutic Agent Delivery Across the Blood–Brain Barrier Using Focused Ultrasound. *Annu. Rev. Biomed. Eng.* **2021**, *23*, 89–113. [CrossRef]

7. Krafft, M.P.; Riess, J.G. Therapeutic oxygen delivery by perfluorocarbon-based colloids. *Adv. Colloid Interface Sci.* **2021**, *294*, 102407. [CrossRef]

8. Duan, L.; Yang, L.; Jin, J.; Yang, F.; Liu, D.; Hu, K.; Wang, Q.; Yue, Y.; Gu, N. Micro/nano-bubble-assisted ultrasound to enhance the EPR effect and potential theranostic applications. *Theranostics* **2020**, *10*, 462–483. [CrossRef]

9. Guo, R.; Xu, N.; Liu, Y.; Ling, G.; Yu, J.; Zhang, P. Functional ultrasound-triggered phase-shift perfluorocarbon nanodroplets for cancer therapy. *Ultrasound Med. Biol.* **2021**, *47*, 2064–2079. [CrossRef]

10. Endo-Takahashi, Y.; Negishi, Y. Microbubbles and nanobubbles with ultrasound for systemic gene delivery. *Pharmaceutics* **2020**, *12*, 964. [CrossRef]

11. Peruzzi, G.; Sinibaldi, G.; Silvani, G.; Ruocco, G.; Casciola, C.M. Perspectives on cavitation enhanced endothelial layer permeability. *Colloids Surf. B Biointerfaces* **2018**, *168*, 83–93. [CrossRef] [PubMed]

12. Escoffre, J.-M.; Bouakaz, A. Minireview: Biophysical mechanisms of cell membrane sonopermeabilization. Knowns and unknowns. *Langmuir* **2019**, *35*, 10151–10165. [CrossRef]

13. An, S.; Ranaweera, R.; Luo, I. Harnessing bubble behaviors for developing new analytical strategies. *Analyst* **2020**, *145*, 7782–7795. [CrossRef] [PubMed]

14. Wang, S.; Hossack, J.A.; Klibanov, A.L. From anatomy to functional and molecular biomarker imaging and therapy: Ultrasound is safe, ultrafast, portable, and inexpensive. *Investig. Radiol.* **2020**, *55*, 559–572. [CrossRef] [PubMed]

15. Park, B.; Yoon, S.; Choi, Y.; Jang, J.; Park, S.; Choi, J. Stability of engineered micro or nanobubbles for biomedical applications. *Pharmaceutics* **2020**, *12*, 1089. [CrossRef]

16. Versluis, M.; Stride, E.; Lajoinie, G.; Dollet, B.; Segers, T. Ultrasound contrast agent modeling: A review. *Ultrasound Med. Biol.* **2020**, *46*, 2117–2144. [CrossRef]

17. Lee, L.; Cavalieri, F.; Ashokkumar, M. Exploring new applications of lysozyme-shelled microbubbles. *Langmuir* **2019**, *35*, 9997–10006. [CrossRef] [PubMed]

18. Shi, D.; Wallyn, J.; Nguyen, D.-V.; Perton, F.; Felder-Flesch, D.; Bégin-Colin, S.; Maaloum, M.; Krafft, M.P. Microbubbles decorated with dendronized magnetic nanoparticles for biomedical imaging: Effective stabilization via fluorous interactions. *Beilstein J. Nanotechnol.* **2019**, *10*, 2103–2115. [CrossRef] [PubMed]

19. Helfield, B. A review of phospholipid encapsulated ultrasound contrast agent microbubble physics. *Ultrasound Med. Biol.* **2019**, *45*, 282–300. [CrossRef]

20. Langeveld, S.A.G.; Schwieger, C.; Beekers, I.; Blaffert, J.; van Rooij, T.; Blume, A.; Kooiman, K. Ligand distribution and lipid phase behavior in phospholipid-coated microbubbles and monolayers. *Langmuir* **2020**, *36*, 3221–3233. [CrossRef]

21. Frinking, P.; Segers, T.; Luan, Y.; Tranquart, F. Three decades of ultrasound contrast agents: A review of the past, present and future improvements. *Ultrasound Med. Biol.* **2020**, *46*, 892–908. [CrossRef]

22. Linder, M.B. Hydrophobins: Proteins that self-assemble at interfaces. *Curr. Opin. Colloid Interface Sci.* **2009**, *14*, 356–363. [CrossRef]

23. Berger, B.W.; Sallada, N.D.J. Hydrophobins: Multifunctional biosurfactants for interface engineering. *Biol. Eng.* **2019**, *13*, 10. [CrossRef] [PubMed]

24. Szilvay, G.R.; Paananen, A.; Laurikainen, K.; Vuorimaa, E.; Lemmetyinen, H.; Peltonen, J.; Linder, M.B. Self-assembled hydrophobin protein films at the air-water interface: Structural analysis and molecular engineering. *Biochemistry* **2007**, *46*, 2345–2354. [CrossRef] [PubMed]

25. Lo, V.C.; Ren, Q.; Pham, C.L.L.; Morris, V.K.; Kwan, A.H.; Sunde, M. Fungal hydrophobin proteins produce self-assembling protein films with diverse structure and chemical stability. *Nanomaterials* **2014**, *4*, 827–843. [CrossRef] [PubMed]

26. Cox, A.R.; Aldred, D.L.; Russell, A.B. Exceptional stability of food foams using class II hydrophobin HFBII. *Food Hydrocoll.* **2009**, *23*, 366–376. [CrossRef]

27. Dokouhaki, M.; Hung, A.; Kasapis, S.; Gras, S.L. Hydrophobins and chaplins: Novel bio-surfactants for food dispersions. *Trends Food Sci. Technol.* **2021**, *111*, 378–387. [CrossRef]

28. Akanbi, M.H.J.; Post, E.; Meter-Arkema, A.; Rink, R.; Robillard, G.T.; Wang, X.; Wösten, H.A.B.; Scholtmeijer, K. Use of hydrophobins in formulation of water insoluble drugs for oral administration. *Colloids Surf. B Biointerfaces* **2010**, *75*, 526–531. [CrossRef]

29. Sarparanta, M.P.; Bimbo, L.M.; Mäkilä, E.M.; Salonen, J.J.; Laaksonen, P.H.; Helariutta, A.M.K.; Linder, M.B.; Hirvonen, J.T.; Laaksonen, T.J.; Santos, H.A.; et al. The mucoadhesive and gastroretentive properties of hydrophobin-coated porous silicon nanoparticle oral drug delivery systems. *Biomaterials* **2012**, *11*, 3353–3362. [CrossRef]

30. Maiolo, D.; Pigliacelli, C.; Sánchez Moreno, P.; Violatto, M.B.; Talamini, L.; Tirotta, I.; Piccirillo, R.; Zucchetti, M.; Morosi, L.; Frapolli, R.; et al. Bioreducible Hydrophobin-Stabilized Supraparticles for Selective Intracellular Release. *ACS Nano* **2017**, *11*, 9413–9423. [CrossRef]

31. Niu, B.; Li, M.; Jia, J.; Zhang, C.; Fan, Y.-Y.; Li, W. Hydrophobin-enhanced stability, dispersions and release of curcumin nanoparticles in water. *J. Biomater. Sci. Polym. Ed.* **2020**, *31*, 1793–1805. [CrossRef] [PubMed]

32. Wang, B.; Han, Z.; Song, B.; Yu, L.; Ma, Z.; Xu, H.; Qiao, M. Effective drug delivery system based on hydrophobin and halloysite clay nanotubes for sustained release of doxorubicin. *Colloids Surf. A Physicochem. Eng. Asp.* **2021**, *628*, 127351. [CrossRef]

33. Pigliacelli, C.; D'Elicio, A.; Milani, R.; Terraneo, G.; Resnati, G.; Baldelli Bombelli, F.; Metrangolo, P. Hydrophobin-stabilized dispersions of PVDF nanoparticles in water. *J. Fluor. Chem.* **2015**, *177*, 62–69. [CrossRef]

34. Milani, R.; Monogioudi, E.; Baldrighi, M.; Cavallo, G.; Arima, V.; Marra, L.; Zizzari, A.; Rinaldi, R.; Linder, M.; Resnati, G.; et al. Hydrophobin: Fluorosurfactant-like properties without fluorine. *Soft Matter* **2013**, *9*, 6505–6514. [CrossRef]

35. Dichiarante, V.; Milani, R.; Metrangolo, P. Natural surfactants towards a more sustainable fluorine chemistry. *Green. Chem.* **2018**, *20*, 13–27. [CrossRef]

36. Ayaz, N.; Dichiarante, V.; Pigliacelli, C.; Repossi, J.; Gazzera, L.; Borreggio, M.; Maiolo, D.; Chirizzi, C.; Bergamaschi, G.; Chaabane, L.; et al. Hydrophobin-coated solid fluorinated nanoparticles for ^{19}F-MRI. *Adv. Mater. Interfaces* **2021**, *9*, 2101677. [CrossRef]

37. Kordts, M.; Kampe, M.; Kerth, A.; Hinderberger, D. Structure Formation in Class I and Class II Hydrophobins at the Air-Water Interface under Multiple Compression/Expansion Cycles. *ChemistryOpen* **2018**, *7*, 1005–1013. [CrossRef]

38. Gazzera, L.; Milani, R.; Pirrie, L.; Schmutz, M.; Blanck, C.; Resnati, G.; Metrangolo, P.; Krafft, M.P. Design of highly stable echogenic microbubbles through controlled assembly of their hydrophobin shell. *Angew. Chem. Int. Ed.* **2016**, *55*, 10263–10267. [CrossRef]

39. de Jong, N.; Hoff, L.; Skotland, T.; Bom, N. Absorption and scatter of encapsulated gas filled microspheres: Theoretical considerations and some measurements. *Ultrasonics* **1992**, *30*, 95–103. [CrossRef]

40. Riccobelli, D.; Al-Terke, H.H.; Laaksonen, P.; Metrangolo, P.; Paananen, A.; Ras, R.H.A.; Ciarletta, P.; Vella, D. Flattened and wrinkled encapsulated droplets: Shape-morphing induced by gravity and evaporation. *Phys. Rev. Lett.* **2023**, *130*, 218202. [CrossRef]

41. Schneider, M.; Arditi, M.; Barrau, M.-B.; Brochot, J.; Broillet, A.; Ventrone, R.; Yan, F. BR1: A new ultrasonographic contrast agent based on sulfur hexafluoride-filled microbubbles. *Investig. Radiol.* **1995**, *30*, 451–457. [CrossRef] [PubMed]

42. Fournier, L.; de La Taille, T.; Chauvierre, C. Microbubbles for human diagnosis and therapy. *Biomaterials* **2023**, *294*, 122025. [CrossRef] [PubMed]

43. Segers, T.; de Jong, N.; Versluis, M. Uniform scattering and attenuation of acoustically sorted ultrasound contrast agents: Modeling and experiments. *J. Acoust. Soc. Am.* **2016**, *140*, 2506–2517. [CrossRef] [PubMed]

44. Mielke, S.; Liu, X.; Krafft, M.P.; Tanaka, M. Influence of semifluorinated alkane surface domains on phase behavior and linear and nonlinear viscoelasticity of phospholipid monolayers. *Langmuir* **2020**, *36*, 781–788. [CrossRef]